Structural Characterization of Hydrogenated Acrylonitrile–Butadiene Rubbers by Pyrolysis Gas Chromatography and Infrared and Nuclear Magnetic Resonance Spectroscopy

Akihiro Kondo, Hajime Ohtani, Yoshio Kosugi, and Shin Tsuge*

Department of Synthetic Chemistry, Faculty of Engineering, Nagoya University, Nagoya 464, Japan

Yoichiro Kubo, Nobuyuki Asada, Hisanori Inaki, and Akira Yoshioka

Nippon Zeon Co., Ltd., Research & Development Center, Kawasaki 210, Japan.
Received December 10, 1987

ABSTRACT: The microstructures of hydrogenated acrylonitrile–butadiene rubbers (NBRs) with various degrees of hydrogenation were investigated by pyrolysis gas chromatography (PyGC) and infrared and nuclear magnetic resonance spectroscopy. Characteristic peaks on the pyrograms by PyGC, specific absorption bands in the IR spectra, and resonance peaks in the ^1H NMR spectra were interpreted in terms of the microstructures of the hydrogenated NBRs. Characteristic peaks in ^{13}C NMR spectra were interpreted in terms of the sequence distribution and hydrogenation mechanisms. PyGC and ^{13}C NMR also supplied good complementary information about longer sequence along the chains and the mechanisms of the hydrogenation reaction.

Acrylonitrile–butadiene rubbers (NBRs) are used for various purposes because of their oil-resistant characteristics. However, NBRs do not have enough heat stability due to the presence of double bonds derived from butadiene (BD) units in the main chain. Hydrogenated NBRs have been developed[1–3] to improve the thermal stability. During the hydrogenation reactions of NBRs, a small number of double bonds are kept unhydrogenated for the subsequent sulfur vulcanization, and all the cyano groups have to be kept unhydrogenated to retain oil resistance. Since the amount and the distribution of the remaining double bonds influence the properties of the hydrogenated NMRs, it is important to characterize their microstructures and the hydrogenation mechanisms. Spectroscopic methods such as IR and NMR are most generally used to investigate polymer microstructures. Furthermore, owing to the recent development of excellent pyrolyzers and highly efficient fused silica capillary columns, pyrolysis gas chromatography (PyGC) has become a powerful tool to give unique information about microstructures of high polymers.[4,5]

In this work, the microstructures of hydrogenated NBRs were investigated by spectroscopic methods such as IR and NMR and by high-resolution PyGC. Degrees of hydrogenation were calculated from the intensities of characteristic peaks in IR and ^1H NMR spectra of the samples, and the results were compared with those determined by an iodine value method. On the other hand, the pyrograms of hydrogenated NBRs were interpreted with regard to the degree of hydrogenation. Moreover, several peaks of larger degradation products were correlated to long sequences in the polymer chain. In addition, newly assigned characteristic peaks in a high-resolution ^{13}C NMR spectrum were interpreted in terms of the sequence distribution and hydrogenation mechanisms.

Experimental Section

Samples. Hydrogenated NBRs were prepared by dissolving NBR in tetrahydrofuran followed by hydrogenation in the presence of palladium catalyst. The samples used in this work are listed in Table I.

Conditions for PyGC. The high-resolution PyGC system utilized in this work was basically the same as that described previously.[6] A vertical microfurnace-type pyrolyzer (Yanagimoto GP-1018) was directly attached to a gas chromatograph (Hewlett-Packard 5890A) with a flame ionization detector (FID). About 70 μg of the sample was pyrolyzed at 550 °C under a flow of nitrogen carrier gas (50 mL/min). Two kinds of fused silica capillary columns (0.25-mm i.d. × 60-m length) with different stationary phases [poly(dimethylsiloxane) and poly((5% phenyl)methylsiloxane)] were used. The carrier gas flow at the pyrolyzer was reduced to 0.5 mL/min at the capillary column by a splitter. The column temperature was programmed from 0 to 300 °C at a rate of 5 °C/min after maintaining at 0 °C for 5 min. The identification of the peaks on the pyrograms was carried out by using a directly coupled gas chromatograph–mass spectrometer with both electron impact (EI) and chemical ionization (CI) sources (Shimadzu QP1000) to which the pyrolyzer was also directly attached. EI mass spectra were obtained at 70 eV with a mass scan range of 33–400 amu. For CI, isobutane was used as the reagent gas, and the mass range of 80–500 amu was scanned.

Table I
NBR and Hydrogenated NBR Samples

no.	notation[a]	degree of hydrogenation[b]
1	N-37(0)	0
2	N-37(44)	44
3	N-37(65)	65
4	N-37(90)	90
5	N-37(95)	95
6	N-37(98)	98
7	N-45(0)	0
8	N-45(90)	90

[a] For example, N-37(44) means a 44% hydrogenated NBR of which the original AN content is 37%. [b] Degrees of hydrogenation of double bonds in the sample determined by the iodine value method.

NMR Spectroscopy. ^{13}C NMR measurements were conducted by using a Varian XL-100 and a JEOL GX-500 NMR spectrometer operating at 25.2 and 125.6 MHz, respectively. The samples were dissolved in chloroform-d_1 to make about 10% (w/v) solutions. Data accumulation conditions at 25.2 MHz were as follows: pulse width, 20 μs; pulse delay, 0.2 s; data points/spectrum, 8192; 40 000 scans; acquisition time, 0.8 s. Those for 125.6 MHz were as follows: 17.5 μs, 13.3 s; 65 536; 100 000 scans; 1.1 s, respectively. ^1H NMR measurements were carried out in the continuous mode by using a JEOL PMX-60 NMR spectrometer at 60 MHz.

IR Spectroscopy. IR spectra were recorded by a JASCO A-202X spectrometer. Sample films were deposited from $CHCl_3$ solution on NaCl plates.

Results and Discussion

Characterization by IR. Figure 1 shows the IR spectra of NBR samples before and after intermediate hydrogen-

0024-9297/88/2221-2918$01.50/0

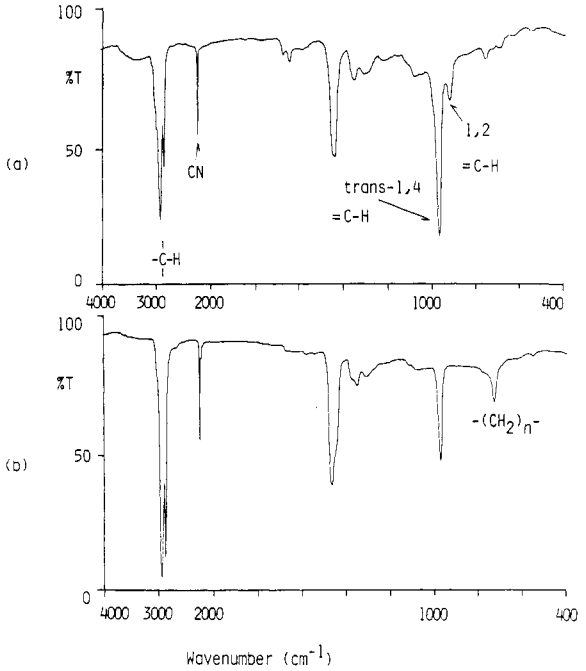

Figure 1. IR spectra of NBRs before and after intermediate hydrogenation: (a) N-37(0); (b) N-37(65).

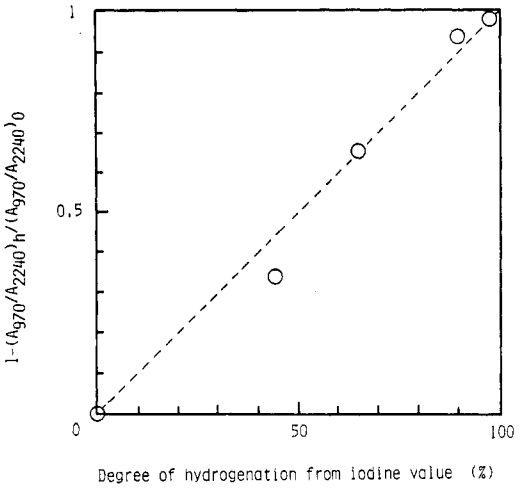

Figure 2. Relationship between observed $1 - [(A_{970}/A_{2240})_h/(A_{970}/A_{2240})_0]$ and degree of hydrogenation for hydrogenated NBRs.

ation ((a) N-37(0) and (b) N-37(65)), where N-37 denotes the acrylonitrile content (37%), and hydrogenation degrees (0%, 65%) are given in parentheses. The absorption by aliphatic C–H stretching (3000–2800 cm^{-1}) and newly appeared $-(CH_2)_n-$ rocking absorption at about 720 cm^{-1} arising from hydrogenated 1,4-BD units increased with the progress of hydrogenation reaction. In contrast, olefinic C–H out-of-plane deformation absorption of *trans*-1,4-BD units at 970 cm^{-1} and those of vinyls (1,2-BD units) at 910 cm^{-1} showed an opposite tendency. The latter almost disappeared at 65% hydrogenation. This fact suggests that pendent vinyl groups are hydrogenated in preference to 1,4-BD units in the polymer main chain. On the other hand, the fact that the absorption of C≡N stretching at about 2240 cm^{-1} little changed in intensity with hydrogenation shows that C≡N groups were hardly reduced under given hydrogenation conditions.

Figure 2 shows the relationship between the degree of hydrogenation estimated from the iodine value and that calculated from the relative IR absorbance ratio $[1 - (A_{970}/A_{2240})_h/(A_{970}/A_{2240})_0]$, where A_{970} and A_{2240} are absorbances at 970 and 2240 cm^{-1}, respectively, and the subscripts 0 and h represent NBR samples before and after hydrogenation, respectively. Although on the whole there exists a fairly good linear correlation between them, the plot in an intermediate hydrogenation slightly shifts to lower value probably because the absorption of 1,2-BD units, which are preferentially hydrogenated, was not taken into account. Furthermore, the absorption at 970 cm^{-1} becomes too weak at more than 90% hydrogenation to determine the degree of hydrogenation accurately at higher regions where hydrogenated NBRs are expected to be used practically.

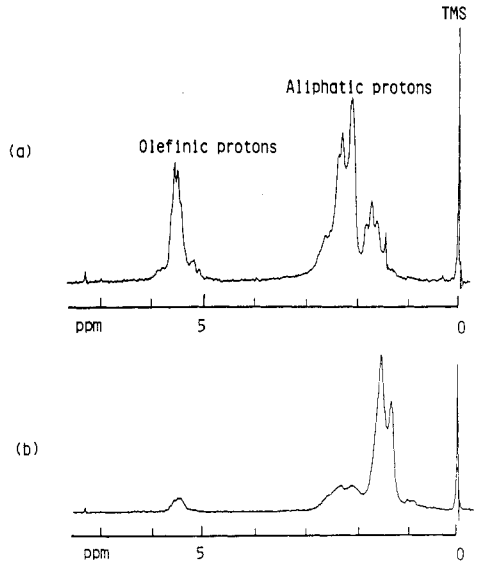

Figure 3. ^1H NMR spectra of NBRs before and after intermediate hydrogenation: (a) N-37(0); (b) N-37(65).

Characterization by ^1H NMR. Figure 3 shows ^1H NMR spectra of NBR samples before and after intermediate hydrogenation ((a) N-37(0) and (b) N-37(65)). Major peaks are observed in the aliphatic (1–3 ppm) and olefinic regions (5–6 ppm). The peak intensity of the former region increased with the progress of hydrogenation while that in the latter region steeply decreased. The degree of hydrogenation can be calculated from the relative intensities of these peaks. Although the composition of the 1,4- and 1,2-units also affects the peak intensity because the ratios of aliphatic and olefinic protons are different in those units, 2:1 for $-CH_2H{=}CHCH_2-$ and 1:1 for $-CH_2CH(CH{=}CH_2)-$, here we assumed only 1,4 type of double bonds remain even at 44% hydrogenation because 1,2-units are preferentially hydrogenated in an earlier stage of the reaction.

Figure 4 shows the relationship between the values thus obtained and those determined by the iodine value method. Although both values nearly agreed, the values from ^1H NMR spectra were always slightly higher than those calculated from iodine values. This fact suggests that the latter might be smaller than the real values. In addition, it is also difficult to determine the degrees of hydrogenation for highly hydrogenated samples since the peaks in the olefinic region become too small to measure accurately.

Characterization by PyGC. Figure 5 shows the pyrograms of NBR samples at 550 °C before and after hydrogenation ((a) N-37(0), (b) N-37(44), and (c) N-37(98)) by using the fused silica capillary column with poly(dimethylsiloxane) stationary phase. Table II summarizes the characteristic thermal degradation products observed on the pyrograms of NBRs and hydrogenated NBRs. Typical mass spectral data of the characteristic degradation products are shown in Table III.

Table II
Characteristic Degradation Products from Hydrogenated NBR

compd class	abbr[a]	structure	sequence[b]
butadiene	BD	$CH_2=CH-CH=CH_2$	B
butadiene dimer (4-vinylcyclohexene)	VC	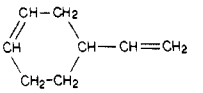	BB
acrylonitrile	AN	$CH_2=CHCN$	A
hydrocarbons	HC	$CH_3(CH_2)_{n-2}CH_3$ $CH_3(CH_2)_{n-3}CH=CH_2$ $CH_2=CH(CH_2)_{n-4}CH=CH_2$	EE ($n \leq 9$) EEE ($n \leq 13$)
mononitriles	MN(A)	$CH_3(CH_2)_{n-2}C\equiv N$ $CH_2=CH(CH_2)_{n-3}C\equiv N$	EA ($n \leq 7$) EEEA ($n \leq 15$)
	MN(B)	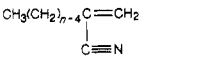	EA ($n \leq 8$) EEA ($n \leq 12$)
	MN(C)	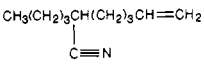	EAE
	MN(D)	$CH_2=CHCH=CHCH_2CH_2C\equiv N$ or $CH_3CH_2CH=CHCH=CHC\equiv N$	BA
dinitriles	DN	$N\equiv C(CH_2)_7C\equiv N$	AEA
		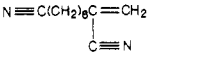	AEA

[a] Abbreviations correspond to those in Figures 5 and 6. [b] B = 1,4-butadiene unit; A = acrylonitrile; E = hydrogenated 1,4-butadiene unit.

Table III
Typical Mass Spectral Data of Characteristic Degradation Products from Hydrogenated NBR

notation	MW[a]	major ion by EI[b]	structure
C_7-MN(A) (unsaturated)	109	41 (100), 55 (30), 54 (20), 68 (14), 69 (14), 80 (14)	$CH_2=CH(CH_2)_4C\equiv N$
C_{11}-MN(A) (unsaturated)	165	41 (100), 55 (86), 122 (38), 39 (34), 136 (30), 69 (28)	$CH_2=CH(CH_2)_8C\equiv N$
C_{10}-MN(A) (saturated)	153	41 (100), 43 (74), 96 (59), 82 (54), 110 (54), 55 (45)	$CH_3(CH_2)_8C\equiv N$
C_7-MN(B)	109	68 (100), 43 (80), 41 (70), 67 (57), 42 (42), 39 (34)	$CH_3(CH_2)_3C(C\equiv N)=CH_2$
C_{11}-MN(B)	165	41 (100), 43 (82), 57 (47), 108 (45), 94 (35), 122 (35)	$CH_3(CH_2)_7C(C\equiv N)=CH_2$
C_{11}-MN(C)	165	41 (100), 94 (60), 109 (55), 108 (38), 55 (35), 54 (33)	$CH_3(CH_2)_3C(C\equiv N)(CH_2)_3CH=CH_2$
C_7-MN(D)	107	41 (100), 92 (55), 79 (49), 80 (49), 107 (49), 52 (43)	$CH_2=CHCH=CHCH_2CH_2C\equiv N$ or $CH_3CH_2CH=CHCH=CHC\equiv N$
C_9-DN	150	41 (100), 92 (55), 79 (49), 80 (49), 107 (49), 52 (43)	$N\equiv C(CH_2)_7C\equiv N$
C_{10}-DN	162	41 (100), 55 (99), 94 (55), 39 (47), 54 (37), 68 (36)	$N\equiv C(CH_2)_6C(C\equiv N)=CH_2$

[a] Determined by CI mass spectra. [b] The relative intensities of major peaks in the mass spectra are given in parentheses.

Characteristic peaks in the pyrogram of N-37(0) are butadiene (BD) monomer, BD dimer, and acrylonitrile (AN) monomer, whereas those of hydrogenated NBR consist of a series of linear mononitriles (MN(A)s) up to C_{12}, each of which consists of a doublet corresponding to an α-olefinic MN(A) (the former) and a saturated MN(A) (the latter).[7] Another series of mononitrile positional isomers (MN(B)s) are also observed. In addition, C_{11} mononitrile (MN(C)) and C_9 and C_{10} dinitriles (DN), which reflect the alternate arrangement of AN and hydrogenated BD units (BD–AN–BD and AN–BD–AN, respectively), are also observed. Moreover, a series of peaks of hydrocarbons (HC) are observed, which reflect the methylene chains produced by hydrogenation. HC peaks of each carbon number consist of a triplet corresponding to an α,ω-diolefin, an α-olefin, and a n-alkane. The fact that up to C_{12}-HC peaks are observed suggests that at least a hydrogenated BD–BD–BD sequence exists in the polymer chain.

On the pyrogram shown in Figure 5, however, the peak of C_6 MN(A) overlaps with that of BD dimer. On the other hand, by use of the column with the stationary phase containing poly((5% phenyl)methylsiloxane), the overlapping peaks were able to be separated on the pyrograms, but in turn some peaks of MN(A) and HC came to overlap as shown in Figure 6. Therefore, only the peak area of the BD dimer was estimated by using the latter separation column while MN(A) and HC were determined with the former one (Figure 5). The peak intensity of BD dimer drastically decreased with the progress of hydrogenation

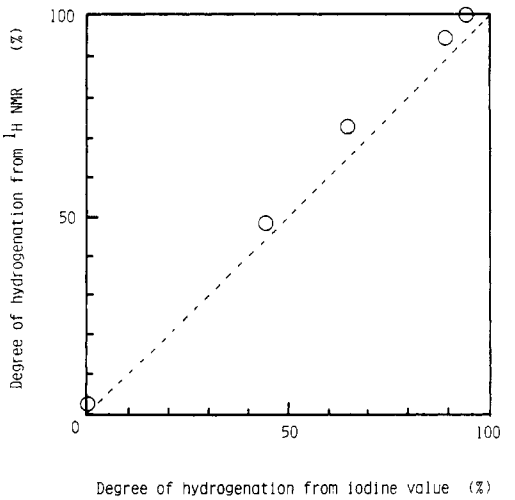

Figure 4. Relationship between degree of hydrogenation of hydrogenated NBRs from iodine value and those determined by ^{1}H NMR.

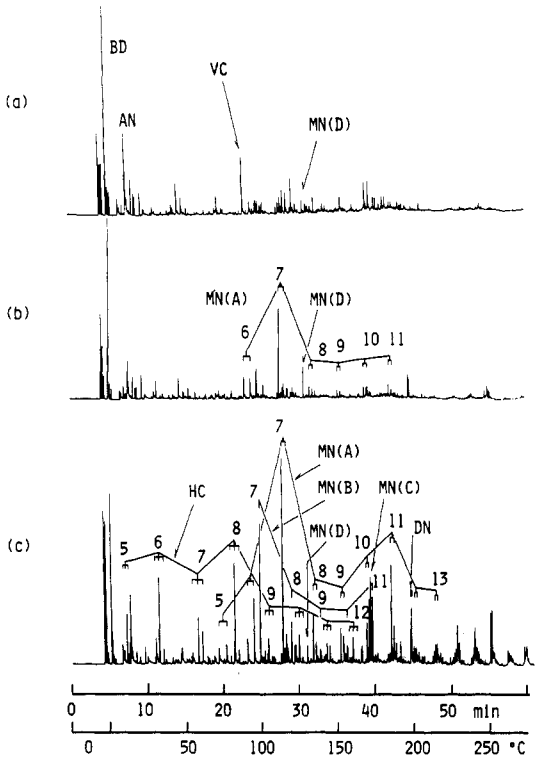

Figure 5. Pyrograms of NBRs before and after hydrogenation at 550 °C separated by a poly(dimethylsiloxane) column: (a) N-37(0); (b) N-37(44); (c) N-37(98). Abbreviations correspond to those in Table II. Numbers indicate carbon numbers of compounds.

and was hardly observed even at 44% hydrogenation. This suggests that the number of unhydrogenated 1,4-BD diads in the polymer chain becomes negligible before 44% hydrogenation.

Among a series of MN(A)s, C_7-MN(A) becomes predominant probably through the following degradation mechanism:

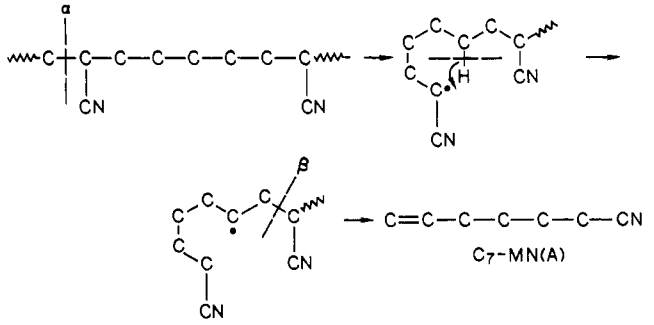

The C–C bond of the α-position of methine carbon is preferentially cleaved, and then the specific intramolecular radical transfer (back-biting) followed by β-scission yields C_7-MN(A),[8] which is likely to occur in a hydrogenated AN–BD–AN sequence. Similarly C_{11}-MN(A) is formed when a hydrogenated AN–BD–BD–AN sequence is subjected to the double back-biting radical transfer followed by β-scission. In fact, the C_{11}-MN(A) peak is the second largest among the peaks of MN(A)s.

Figure 7 shows the relationships between the degree of hydrogenation determined by the iodine value method and the peak area of C_7-MN(A) and C_{11}-MN(A) normalized with the sample weight (micrograms). Both curves clearly represent monotonously increasing correlation even for the highly hydrogenated samples that are practically used. Among these two curves, that for C_7-MN(A) could be

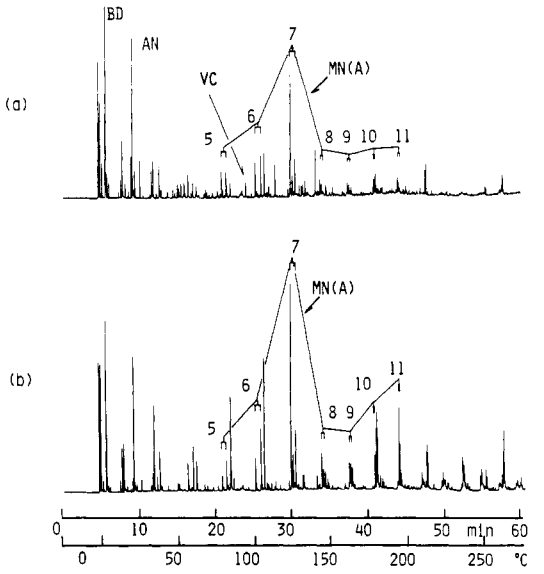

Figure 6. Pyrograms of hydrogenated NBRs at 550 °C separated by a poly((5% phenyl)methylsiloxane) column: (a) N-37(44); (b) N-37(98). Abbreviations correspond to those in Table II. Numbers indicate carbon numbers of compounds.

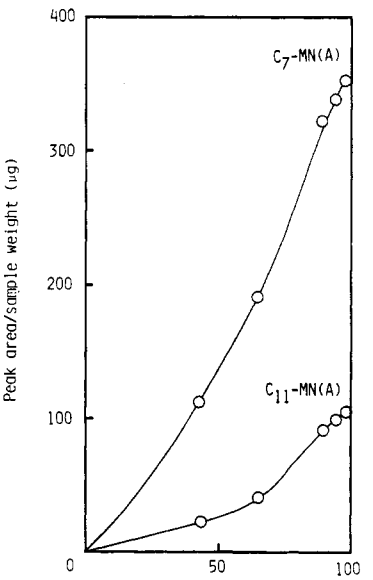

Figure 7. Relationships between observed peak intensities of C_7 mononitrile(A) (C_7-MN(A)) and C_{11} mononitrile(A) (C_{11}-MN(A)) and degree of hydrogenation for hydrogenated NBRs.

better used as a practical calibration curve since the increments of the peak intensity at the higher hydrogenation region are much larger than those for C_{11}-MN(A).

On the other hand, the formation of MN(B)s are associated with the cleavage at the β-position of methine carbon:

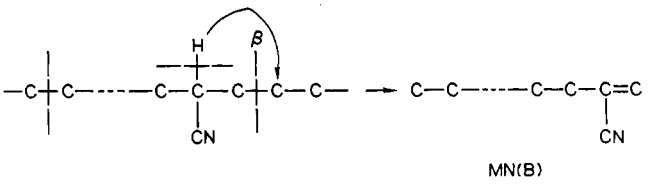

Among these MN(B)s, the predominant C_7 MN(B) may also be given through the following back-biting mechanism on the hydrogenated AN-BD-AN sequence:

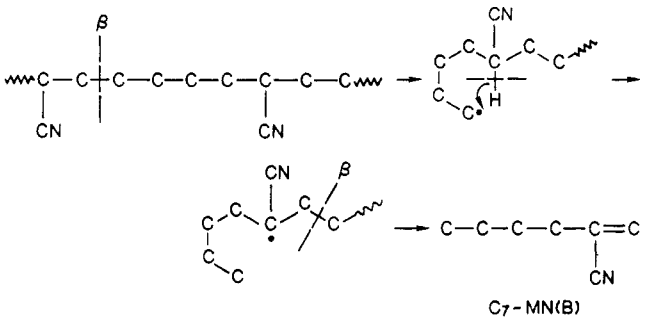

Furthermore, C_{11}-MN(B)s are also formed through the double back-biting mechanism on the hdyrogenated AN–BD–BD–AN sequence. The formations of MN(C) and DN are interpreted in terms of the cleavages in a hydrogenated sequence with alternating AN and BD units as follows:

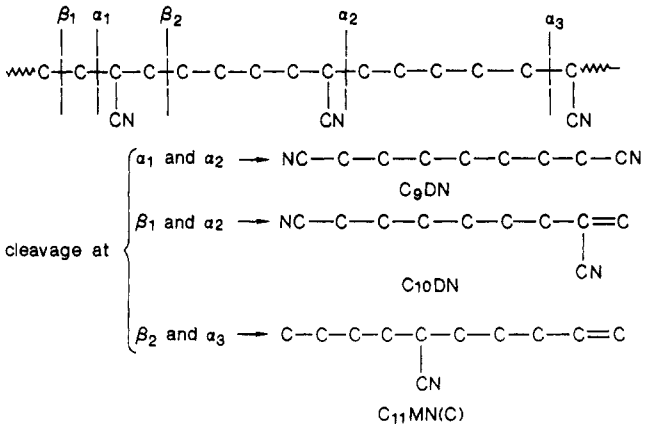

Figure 8 shows the detailed pyrograms of two kinds of hydrogenated NBRs with different acrylonitrile contents: (a) N-37(90) and (b) N-45(90). For the sample of higher acrylonitrile content (b), C_{11}-MN(C) and C_9- and C_{10}-DNs, which reflect hydrogenated BAB and ABA sequences, respectively, are predominant, whereas C_{10}- and C_{11}-MN(A), which reflect an ABB sequence, become comparably strong for N-37(90).

On the other hand, as shown in Figure 9, it is interesting to note that the peak intensity of MN(D) indicates a maximum around the intermediate stage of hydrogenation. From the mass spectral data, the molecular formula of MN(D) is defined as C_7H_9N (MW = 107). The fact that the retention time of the peak of MN(D) on the pyrogram is considerably later than that of monoolefinic C_7-MN(A) (MW = 109) suggests that the MN(D) should contain conjugated double bonds. Therefore, this characteristic product can be assigned to CH_2=$CHCH$=$CHCH_2CH_2CN$ or CH_3CH_2CH=$CHCH$=$CHCN$, which are associated with the sequences consisting of one BD and one AN unit.

The possible MN(D)s with conjugated double bonds might be formed through the cleavages of two α-positions (α_1 and α_2) in the unhydrogenated alternating AN-BD sequence as follows:

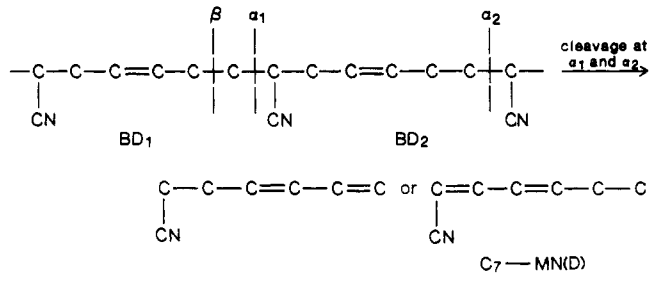

In the case of unhydrogenated NBR, the cleavage of β followed by depolymerization reaction predominantly occurs rather than that at α_1. When the BD_1 unit is hydrogenated, however, the contribution of the cleavage at α_1 becomes significant while that at β becomes less significant. At the final stage of hydrogenation, the BD_2 unit is also hydrogenated and thus MN(D) is scarcely formed. Therefore, between two extreme degrees of hydrogenation, there exists a point to give a maximum yield for MN(D) that mainly reflects the hydrogenated BD–AN–unhydrogenated BD sequence.

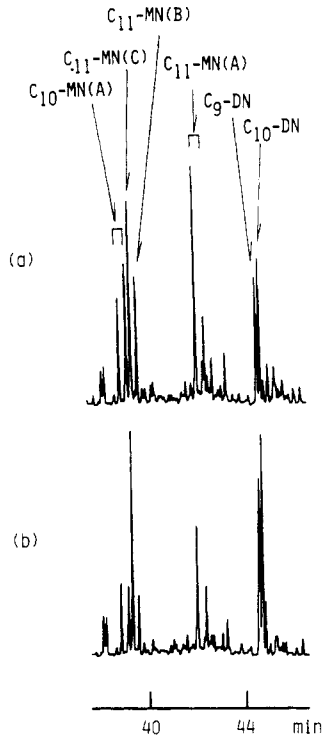

Figure 8. Detailed pyrograms of hydrogenated NBRs with different acrylonitrile contents: (a) N-37(90); (b) N-45(90). Notations correspond to those in Table III.

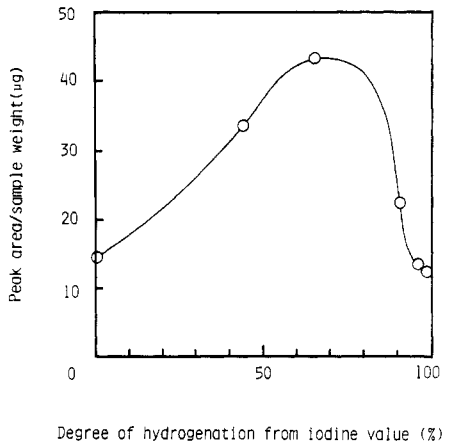

Figure 9. Relationship between observed peak intensity of mononitrile(D) (MN(D)) and degree of hydrogenation for hydrogenated NBRs.

Characterization by ^{13}C NMR. Figure 10 shows the 25.2-MHz ^{13}C NMR spectra of 90% hydrogenated NBR samples with two kinds of acrylonitrile contents: (a) N-37(90) and (b) N-45(90). Peaks of aliphatic and CN carbons are mainly observed, while peaks of 10% remaining olefinic carbons are diversely observed over a wide range of chemical shifts corresponding to various possible sequences containing BD, AN, and hydrogenated BD units. In the previous works, the peaks in the aliphatic region

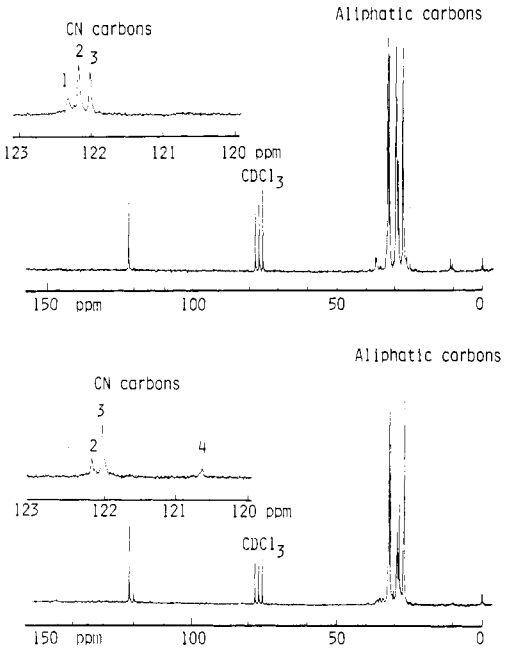

Figure 10. 25.2-MHz ^{13}C NMR spectra of hydrogenated NBRs ((a) N-37(90); (b) N-45(90)) and expanded spectra of CN regions. Peaks 1–4 are assigned in Table IV.

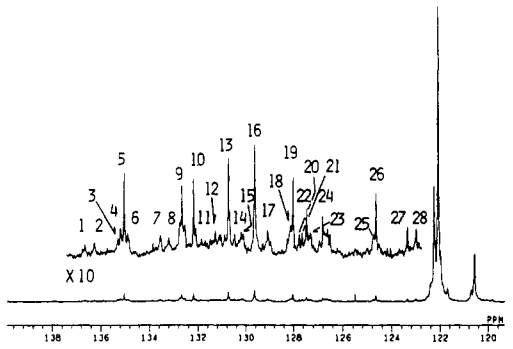

Figure 11. 125-MHz ^{13}C NMR spectrum in olefinic region of a hdyrogenated NBR sample (N-45(90)). Peak assignments are listed in Table V.

Table IV
Amounts of Pentads Containing CN Units in Hydrogenated NBR Determined by ^{13}C NMR Spectra

peak no.[a]	assignment	pentad[b]	P_5(--A--)[c] N-37(90)	P_5(--A--)[c] N-45(90)
1	-CCCCCCCCCCCCCCCCC- (CN)	EEAEE	0.20	0.04
2	-CCCCCCCCCCCCCCCCC- (CN, CN)	EEAEA	0.47	0.24
3	-CCCCCCCCCCCCCCC- (CN, CN, CN)	AEAEA	0.33	0.62
4	-CCCCCCCCCCCC- (CN CN)	EEAAE AEAAE		0.10

[a] Peak numbers correspond to those in Figure 10. [b] A = acrylonitrile unit; E = hydrogenated butadiene unit. [c] P_5(EEAEE) + P_5(EEAEA) + P_5(AEAEA) + P_5(EEAAE) + P_5(AEAAe) = 1.

on ^{13}C NMR spectra of a completely hydrogenated NBR have been assigned by using model compounds and the additive rule.[9]

The assignments of CN and olefinic peaks are done in the present work. The expanded 25.2-MHz spectra of CN regions are shown in the upper part of the corresponding spectra. Four main peaks are assigned as shown in Table IV on an assumption that the pentad with more AN units is more predominant in N-45(90) and is at a higher field. Alternating sequences are predominant in N-45(90) while relatively random sequences are observed in N-37(90). Thus, these characteristic peaks of AN unit provide useful information on sequence analysis.

Table V
Peak Assignment of the Olefinic Region of ^{13}C NMR Spectra of a Hydrogenated NBR (N-45(90))

peak no.[a]	chem shift, ppm obsd	chem shift, ppm calcd	assignment[b]
1	136.52		unknown
2	136.13		unknown
3	135.17		unknown
4	135.06		unknown
5	134.90	134.23	ABEA
6	134.77	134.73	ABEB, ABEE
7	133.42		unknown
8	133.06		unknown
9	132.62–132.39		ABA
10	132.06	131.46	AEBA
11	131.96	131.96	BEBA, EEBA
12	131.15		unknown
13	130.60	130.37	AEBE, AEBB
14	130.34		unknown
15	130.05	130.12	EtBA
16	129.50	129.87	AEBE, AEBB
17	128.94		unknown
18	127.97	128.12	BEBA, EEBA
19	127.89	128.12	AEBA
20	127.62		unknown
21	127.52		unknown
22	127.34		unknown
23	127.15	127.43	EtBA
24	126.83–126.39		ABA
25	124.65	124.81	ABEB, ABEE
26	124.52	124.81	ABEA
27	123.24		unknown
28	122.87		unknown

[a] Peak numbers correspond to those in Figure 11. [b] A = acrylonitrile unit; B = 1,4-butadiene unit; E = hydrogenated 1,4-butadiene unit; Et = hydrogenated 1,2-butadiene unit.

Table VI
Peak Intensities of Olefinic Carbons in ^{13}C NMR Spectra of NBR before and after Hydrogenation

NBR (N-45(0))[a] triad or tetrad	%	hydrogenated NBR (N-45(90))[a] triad or tetrad	%
ABAA	7.4	ABAA	0.0
		AEAA[b]	7.2
ABA	68.5	ABA	0.8
		AEA[b]	66.5
ABBA	10.4	ABBA	0.0
		ABEA	1.2
		AEEA[b]	8.6
ABBB	6.6	ABBB	0.0
		AEBB	0.7
		ABEB	0.3
		AEEE[b]	5.4
VBA	2.3	VBA	0.0
		EtBA	0.1
		EtEA[b]	2.2
VABA	3.6	unknown peaks	7.0
VBB	1.2		

[a] A = acrylonitrile unit; B = 1,4-butadiene unit; V = 1,2-butadiene unit; E = hydrogenated 1,4-butadiene unit; Et = hydrogenated 1,2-butadiene unit. [b] Intensities were calculated from those of olefinic peaks: $I_{HyNBR}(Y) = I_{NBR}(X) - I_{HyNBR}(X) - I_{NBR}(X)/100 \cdot [I_{HyNBR}(unknown) - I_{NBR}(VABA) - I_{NBR}(VBB)]$, where I_{NBR} and I_{HyNBR} represent the intensities in the spectra of NBR and hydrogenated NBR, respectively, X is the sequence containing unhydrogenated units, and Y is the completely hydrogenated sequence corresponding to X.

Figure 11 shows a 125-MHz ^{13}C NMR spectrum of the olefinic region for a hydrogenated NBR (N-45(90)). A number of peaks observed are assigned as shown in Table V on the basis of the previous assignments for NBR[10] and the chemical shift parameters.[11,12] There are good agreements between the observed and the calculated chemical shifts of main peaks. The intensities of these peaks before and after hydrogenation are given in Table VI. The fact that ABBB sequences are hydrogenated to AEBB 2 or more times more easily than to ABEB suggests that 1,4-BD units adjacent to AN units are preferentially hydrogenated.

Conclusion

The microstructural change of NBRs during the hydrogenation reaction was studied by means of PyGC, IR, and ^1H and ^{13}C NMR. Specific absorption bands in the IR spectra, resonance peaks in the ^1H NMR spectra, and characteristic peaks on the pyrograms by PyGC proved to be good measures for tracing the degree of hydrogenation reaction. Among these, the peak intensity of C_7-MN(A) by PyGC provided a practical calibration curve applicable even to highly hydrogenated NBRs. On the other hand, the IR spectra of various hydrogenated NBRs suggested a preferential hydrogenation reaction of 1,2-BD units over 1,4-units. PyGC and ^{13}C NMR also supplied good complementary information about longer sequences along the chains and the mechanisms of the hydrogenation reaction. The ^{13}C NMR spectra suggested that the BD units next to the AN units in the polymer chain were more likely to be hydrogenated than those next to the same units (BD).

References and Notes

(1) Weinstein, A. H. *Rubber Chem. Technol.* **1984**, *57*, 203.
(2) Mohammadi, N. A.; Rempel, G. L. *Macromolecules* **1987**, *20*, 2362.
(3) Kubo, Y.; Hashimoto, K.; Watanabe, N. *Kautsch. Gummi Kunstst.* **1987**, *40*, 118.
(4) Tsuge, S.; Ohtani, H. *Applied Polymer Analysis and Characterization*; Verlag Chemie: Weinheim, 1986; p 217.
(5) Tsuge, S. *Chromatogr. Forum* **1986**, *1*, 44.
(6) Ohtani, H.; Kimura, T.; Tsuge, S. *Anal. Sci.* **1986**, *2*, 179.
(7) Ohtani, H.; Nagaya, T.; Sugimura, Y.; Tsuge, S. *J. Anal. Appl. Pyrolysis* **1982**, *4*, 117.
(8) Ohtani, H.; Tsuge, S.; Ogawa, T.; Elias, H.-G. *Macromolecules* **1984**, *17*, 465.
(9) Kodama, K.; Yoda, R.; Tanaka, Y. *Polym. Prepr. Jpn.* **1981**, *30*, 2240.
(10) Kodama, K.; Shimoda, M.; Asada, N. *Prepr. Annu. Meet. Jpn. Soc. Anal. Chem.* **1985**, 363.
(11) Elgert, K.-F.; Quack, G.; Stützel, B. *Polymer* **1975**, *16*, 154.
(12) Segre, A. L.; Delfini, M.; Conti, F.; Boicelli, A. *Polymer* **1975**, *16*, 338.

A NMR Study of Miscible Blends in Concentrated Solution. 1. Poly(vinyl methyl ether)/Polystyrene

Molly W. Crowther,* Israel Cabasso,† and George C. Levy

Department of Chemistry, Syracuse University, Syracuse, New York 13210.
Received November 20, 1987

ABSTRACT: High-resolution proton spectra of the miscible polymer blend polystyrene/poly(vinyl methyl ether) (PS/PVME) in concentrated solution have been used to examine intermolecular interactions. The spectral resolution achieved in solution allows the polymer components and the chemically different types of protons within each component to be well resolved. A one-dimensional cross-relaxation experiment shows that the polymers are intimately mixed in toluene solution but not in chloroform. The minimum concentration where magnetization exchange between the polymer pair (in toluene) can be observed lies between 30 and 40 wt % total polymer, of which 50 wt % is polystyrene. The chemical shift difference between the methine and methoxy resonances of PVME is found to vary with the mole ratio of PVME to the total aromatic functionality, from either PS or toluene. Line width vs temperature measurements seem to indicate hindrance of motion for the blend in toluene at elevated temperatures, as the gross phase separation is approached, that is not observed for the pure homopolymer. A two-dimensional exchange experiment was performed at a series of mixing times to measure the intra- and intermolecular spin-diffusion rates. Specific intermolecular rates could not be differentiated in the presence of the very fast intramolecular distribution of the magnetization via spin diffusion.

Introduction

Physical blending of polymers offers a new route to interesting properties and products.[1] Although the possible number of combinations is endless, only very few polymer pairs form miscible blends. The thermodynamic reason for incompatibility is an endothermic free energy of mixing associated with a diminishing contribution, with increasing molecular weight, of the entropy term.[2] Therefore, mixing of polymers is enthalpy-driven and thus favorable intermolecular interactions must exist for a polymer pair to be "compatible". The ongoing quest for the specific interactions responsible for miscibility on the microscopic level, which ultimately affect macroscopic behavior, can be greatly assisted by high-resolution nuclear magnetic resonance (NMR) spectroscopy.

NMR is particularly useful for examining miscibility at the molecular level. Magnetization transfer between nuclei by dipolar interactions has a distance dependence of $1/r^6$.[3] Thus, microhomogeneity in a blend can be demonstrated by the exchange of magnetization from one polymer to the other. This has been observed in the solid state by both one- and two-dimensional techniques via proton–proton,[4-7] proton–carbon,[8-10] proton–fluorine,[11] carbon–fluorine,[12] and carbon–carbon[13-15] dipolar interactions.

The purpose of the present study is to examine polymer–polymer interactions for blends in concentrated solution for which there are limited experimental data. A strong motive establishing the study of polymer blends in solution is the broad availability and experimental simplicity of solution NMR compared to solid state. Although

† Department of Chemistry, State University of New York—ESF, Syracuse, NY 13210.

0024-9297/88/2221-2924$01.50/0